MOL PHARM

MOLECULAR PHARMACOLOGY

aspet

Molecular Docking of Competitive Phosphodiesterase Inhibitors

ORLY DYM, IOANNIS XENARIOS, HENGMING KE, and JOHN COLICELLI

University of California Los Angeles-Department of Energy Laboratory of Structural Biology and Molecular Medicine, University of California Los Angeles, Los Angeles, California (O.D., I.X.); Department of Biochemistry and Biophysics, University of North Carolina at Chapel Hill, Chapel Hill, North Carolina (H.K.); and Department of Biological Chemistry and the Molecular Biology Institute, University of California Los Angeles School of Medicine, Los Angeles, California (J.C.)

ABSTRACT

Mammalian phosphodiesterases types 3 and 4 (PDE3 and PDE4) hydrolyze cAMP and are essential for the regulation of this intracellular second messenger. These enzymes share structural and biochemical similarities, but each can be distinguished by its sensitivity to isoenzyme-specific, substrate-competitive inhibitors. We present a model configuration for the PDE4 substrate (cAMP) and a PDE4-specific inhibitor (rolipram) within the active site of the enzyme. The docked models were also used to examine the structural consequences of mutations that confer resistance to rolipram and other PDE4-specific inhibitors. The proposed rolipram-binding configuration is consistent with the substrate-competitive nature of inhibition and also provides a structural basis for the observed specificity of binding to the *R*- versus *S*-enantiomer. For mutations that render the enzyme rolipram-insensitive, there was generally an inverse relationship between the magnitude of the drug resistance and the distance of the altered residue from the predicted binding site. We observed a direct correlation between the net loss of protein residue interactions (van der Waals contacts and hydrogen bond interactions) and the degree of rolipram resistance. The positions of several drug sensitivity-determinant residues define a surface leading to the substrate- and drug-binding sites, suggesting a possible approach channel leading to the enzyme active site. The binding of other PDE4 inhibitors (high- and low-affinity) was also modeled and used to predict the involvement of residues that were not previously implicated in pharmacological interactions.

cAMP is a ubiquitous intracellular second messenger. Its effects are principally mediated through the indirect activation of cAMP-dependent protein kinases. There are families of enzymes that regulate cAMP synthesis (adenylyl cyclases) and cAMP degradation [phosphodiesterases (PDEs)] (Houslay and Milligan, 1997). The mammalian PDEs have been categorized into 11 types relating to their substrate selectivity, kinetics, and pharmacological sensitivity (Francis et al., 2000; Soderling and Beavo, 2000). PDEs across families share considerable sequence similarity. Confined primarily to the catalytic domain, these conserved residues are likely to have direct or indirect involvement in cyclic nucleotide hydrolysis (Jin et al., 1992; Jacobitz et al., 1997; Owens et al., 1997). Within PDE families, sequence identity is more extensive, reflecting greater relatedness in their biochemical properties. PDEs are clinical targets for a range of biological disorders, such as congestive heart failure, asthma, chronic obstructive pulmonary disease, depression, retinal degrada-

tion, and inflammation (Conti et al., 1991; Teixeira et al., 1997; Barnette and Underwood, 2000; Spina, 2000). There is a particular interest in the enzymes encoded by PDE4 genes (PDE4A, PDE4B, PDE4C, and PDE4D) in the search for therapeutically useful inhibitors (Raeburn et al., 1994; Cohan et al., 1996; Holbrook et al., 1996). Rolipram (4-[3-(cyclopentyloxy)-4-methoxyphenyl]-2-pyrrolidinone) is one of the earliest and most extensively studied PDE4 inhibitors. It has an IC$_{50}$ of approximately 1 μM (lower under some conditions) and shows at least a 100-fold selectivity for this PDE family. Indeed, sensitivity to rolipram has become a defining feature of these isozymes. As with other PDE inhibitors, enzymatic inhibition is competitive with substrate. Attempts to identify determinants of substrate- and inhibitor-binding within PDE4 have included a variety of deletion, chimera, and directed point-mutation studies (Jin et al., 1992; Pillai et al., 1993; Atienza et al., 1999). In addition, an approach of random mutagenesis coupled with rolipram-resistance selection has been used to identify drug-specificity determinants within PDE4 (Pillai et al., 1993; Atienza et al., 1999). These mutant enzymes display different degrees of sensitivity to

ABBREVIATIONS: PDE, phosphodiesterases; RP 73401, 3-cyclopentyloxy-*N*-(3,5-dichloropyridin-4-yl)-4-methoxybenzamide; IBMX, 3-isobutyl-1-methylxanthine.

rolipram, as measured by IC_{50} determinations and, in some cases, drug binding assays. Among the studied PDE4 mutants, W406R, M411K, E427G, C432G, V439L, V444E, G445S, I450T, and V451L showed a slight reduction in sensitivity to rolipram, whereas I410T, I410N, D241A, D241N, Y403C, T407A, and F414S were affected more dramatically. In the present study, we performed automated docking of the cAMP substrate and rolipram inhibitor using the known three-dimensional structure of the catalytic domain of human PDE4B (Xu et al., 2000) to understand the inhibition effect of rolipram. Molecular modeling of these PDE4 mutants on the docked models was conducted to better understand their different degrees of resistance to rolipram. The resulting model was used to examine other PDE4 inhibitors. These studies may facilitate the design of therapeutically useful compounds, as well as predict the involvement of residues not previously implicated in pharmacological interactions.

Experimental Procedures

The three-dimensional structure of human PDE4B and cAMP were retrieved from the Protein Data Bank (http://www.rcsb.org/pdb; accession codes 1F0J and 1NHK, respectively). Mark W. Orme provided (R)-rolipram coordinates. Automated docking simulation was implemented to dock cAMP and rolipram into the active site of PDE4 with the program AutoDock version 3.03 (http://www.scripps.edu/pub/olson-web/doc/autodock/; Goodsell et al., 1996; Morris et al., 1998) using the Lamarckian genetic algorithm (Morris et al., 1998). This method has been previously shown to produce binding modes similar to the experimentally observed modes (Goodsell et al., 1996; Sippl, 2000). AutoDock uses a simulated annealing procedure to explore the binding possibilities of a ligand in a binding pocket. The interaction energy of ligand and protein is evaluated using atom affinity potentials calculated on a grid (Goodford, 1985). All ligand atoms but no protein atoms were allowed to move during the docking simulation. Before the docking procedure, water molecules and heteroatoms (magnesium and zinc ions) were removed from the protein crystal structure. Atomic volume and atomic salvation parameters were assigned to the protein molecule using the default values. Hydrogen bonds were added, and partial atomic charges of PDE4, cAMP, and rolipram were assigned using the program Insight II (version 3.0; http://www.msi.umn.edu/bscl/tutorials/insight). The atomic interaction energy grids for cAMP and rolipram were calculated using probes corresponding to each atomic type (C, N, and O) found in these ligands. An atomic energy grid for the protein was produced using the Lennard-Jones coefficients with 12-6 parameters for all types of hydrogen atoms (polar and nonpolar). The grid map consists of 60 points in each x, y, and z direction equally spaced at 0.375 Å. cAMP and rolipram were each docked into the active site of PDE4 and the simulations were composed of 100 docking runs, each of 50 cycles containing a maximum of 10,000 accepted and rejected steps. The simulated annealing procedure was started at high temperature (RT = 616 kcal/mol, where R is the gas constant and T is the steady state temperature) and was decreased by a factor of 0.95 on each cycle. The 100 docked complexes were clustered with a root-mean-square deviation tolerance of 1 Å. The program generated 100 rolipram- and cAMP-docked conformers corresponding to the lowest-energy structures. A detailed inspection of the independent cAMP conformers revealed that most (61%) had nearly identical orientation. Although only one third of the rolipram conformers have the same orientation, the remaining were situated too close (≤2 Å) to residues in the active site. One conformer from each cAMP and rolipram cluster was adopted as the "consensus" structure and used for further analysis. The atomic coordinates of the consensus cAMP and rolipram models have been deposited in the Protein Data Bank

(http://www.rcsb.org/pdb; accession codes 1JP1 and 1JP2, respectively).

Side chains in the wild-type protein were altered to those in each mutant (Table 1) by using the rotamer library in the O software (http://alpha2.bmc.uu.se/~alwyn/o_frameset.html; Wallace et al., 1995). Alternate orientations were tested, but they were ruled out because of geometric clashes with neighboring protein residues. cAMP and rolipram were docked into the active site of each of the refined PDE4 mutant structures, as described above. In addition, van der Waals interactions and electrostatic contacts between cAMP or rolipram and neighboring amino acid side chains were calculated using the program LigPlot (http://www.biochem.ucl.ac.uk/bsm/ligplot/ligplot.html; Wallace et al., 1995).

Results and Discussion

The PDE4B structure is composed of 17 α-helices that form three subdomains (Xu et al., 2000). A deep pocket in the center of the carboxyl-terminal subdomain extends to the junction of the three subdomains. The most highly conserved residues across all PDE family members lie near this pocket. The pocket has a volume of 440 Å^3, large enough to accommodate molecules with sizes comparable with that of cAMP. A comparison of the 100 independent cAMP conformers, obtained using the automated program AutoDock, revealed that 61 of them have nearly identical orientation (Fig. 1A). However, the rest of the conformers are positioned too close (≤2 Å) to at least one of the following residues at the active site: Leu303, Glu304, His307, Thr345, and/or Cys499. Furthermore, the same cluster of conformers was obtained when an alternate cAMP conformation was used as a starting model in the docking procedure. The cluster of the docked cAMP conformers is similar to that of the previously proposed model using the program Ligand Fit (http://www.accelrys.com/support/life/relnotes/RN_C2-30.html) (Xu et al., 2000) with comparable hydrogen bond distances between protein residues and cAMP atoms [obtained using the program LigPlot (Wallace et al., 1995)]. In both models, cAMP adopts the anticonformation with the adenine base inserted into a lipophilic pocket formed by Asp392, Leu393, Pro396, and Ile410. In addition, Tyr233, His234, His238, Thr407, and Cys499 are also found in the active site pocket. Some of the mutations selected for resistance to rolipram (Pillai et al., 1993; Atienza et al., 1999) directly interact with cAMP atoms, whereas others are in the vicinity of the binding pocket. Next, rolipram was positioned in the active site using the

TABLE 1
Distance to the closest PDE4 residue and substrate/inhibitor effects for PDE4 with large changes in rolipram sensitivity (Atienza et al., 1999; Pillai et al., 1993)

Substrate K_m, change in IC_{50} (compared with wild-type), and closest distance between wild-type side chain and the docked drug, as obtained by the AutoDock program, are indicated.

	K_m cAMP	Fold ΔIC_{50} for Rolipram	Distance	
			cAMP	Rolipram
	μm		Å	
PDE4BΔwt	2			
D241A	7	390	7.0	7.0
D241N	3	270		
I410T	340	260	3.0	3.0
I410N	1200	910		
T407A	18	330	4.0	2.8
Y403C	19	8	5.5	4.3
F414S	25	8	6.3	3.5

above-described automated docking procedure. Approximately one third of the rolipram conformers had a similar orientation (Fig. 1B), whereas 20 other conformers are located too close to at least one of the following residues situated at the active site: His274, His278, Ser282, Asp329, and/or Pro346. The remaining rolipram conformers (~50) are positioned too near either Glu413 or Cys499 residues. A more detailed model of rolipram with potential hydrogen bond and hydrophobic interactions to PDE4 residues is illustrated in Fig. 2,, A and B. Remarkably, the cluster of rolipram conformers is positioned in the same general location as the above docked cAMP cluster, with the cyclopentyloxy moiety superimposed on the ribose moiety of cAMP. A superposition of clusters of cAMP and rolipram models is shown in Fig. 1C, and superposition of the consensus cAMP and rolipram docked in the PDE4 active site is shown in Fig. 3.

Side chains in the wild-type protein were then altered to those in the rolipram-resistant mutants (Pillai et al., 1993; Atienza et al., 1999). The side chain rotamers were carefully chosen to minimize clashes with neighboring residues. When the docking procedure was performed on the mutated structures, the clusters of cAMP and rolipram conformers corresponded well to the conformations obtained for the wild-type enzyme. In addition, van der Waals interactions and electrostatic contacts of native and mutated residues with their neighboring residues, in the presence of either cAMP or rolipram (consensus structure), were calculated using the program LigPlot (Wallace et al., 1995). Among the studied PDE4 mutants, M411K, E427G, C432G, V439L, V444E, G445S, I450T, and V451L (wild-type residues depicted with green in Fig. 3) showed a slight reduction in sensitivity to rolipram, whereas I410T, I410N, D241A, D241N, Y403C, T407A, and F414S (Pillai et al., 1993; Atienza et al., 1999; wild-type residues depicted with red in Fig. 3) were more dramatically affected (Table 1).

Inspection of hydrophobic and electrostatic interactions between PDE4 residues and the docked cAMP or rolipram atoms revealed that rolipram forms more contacts than does cAMP. Some of these residues interact with both cAMP and rolipram (Asp392, His238, Tyr233, Ile410, Cys499, and His234), whereas others interact preferentially with one or the other. One of these residues, Phe414, is highly conserved among PDE family members (only PDE8 and PDE9 differ, with Tyr at this position). It is situated significantly closer to rolipram than to cAMP (3.5 Å versus 6.3 Å; Table 1) and

forms hydrophobic contacts with rolipram atoms (Fig. 2, A and B). In addition Phe414 forms extensive hydrophobic and hydrogen bond interactions with neighboring residues. However, when Phe414 is replaced with Ser, some of these interactions are lost. Moreover, rolipram is 7.5 Å away from the Ser side chain, too great a distance for productive contacts. This observation is consistent with previous results indicating that this substitution reduces rolipram binding by 8-fold (Atienza et al., 1999). A more potent effect was observed for I410T and I410N mutations. Ile410, another conserved residue (Ile, Leu, or Val in all PDEs), displays hydrophobic contacts with several rolipram atoms as well as with the protein residues Tyr233 and Thr407. It also has electrostatic interactions with Arg409, Met411, and Phe414. When Ile410 is mutated to Thr or Asn, the hydrophobic interactions to atoms in Thr407 and rolipram are lost. This is in agreement with the large reduction in rolipram sensitivity observed for I410T and I410N mutants (260- and 900-fold, respectively). Another consequence of these disruptions and of the close proximity of Ile410 to docked cAMP is that both the I410T and I410N mutants showed a dramatic increase in K_m values (Table 1).

The T407A mutation also caused a dramatic reduction in rolipram binding (19-fold) and IC$_{50}$ (330-fold) (Pillai et al., 1993). From our docked models, the Thr side chain is approximately 4.0 Å from cAMP but only 2.8 Å from rolipram. The O_1 atom from the pyrrolidinone moiety is within hydrogen-bonding distance to OG_1 of Thr407 (Fig. 4). However, when Thr407 is replaced by Ala, this electrostatic interaction is lost, along with an electrostatic interaction between the OH group of Tyr480 and the OG_1 atom from Thr407. The same phenomenon, a net loss of contact strength, is observed for all of the mutations that confer the most dramatic reduction in rolipram sensitivity (D241A, D241N, I410T, I410N, T407A, Y403C, and F414S, colored red in Fig. 3). Remarkably, these key residues are all located around the binding site with their side chains directed toward the center. In contrast, mutations that confer less resistance, as mentioned above, tend to be located at some distance from the active site and are out of range for direct contact with the inhibitor (wild-type residues are colored green in Fig. 3). Consequently, the interactions between these residues (wild-type or mutated) and neighboring side chains are essentially identical when cAMP or rolipram are placed in the active site. Our model also predicts that PDE4 residues, Asn395, His234, Cys499, Tyr233,
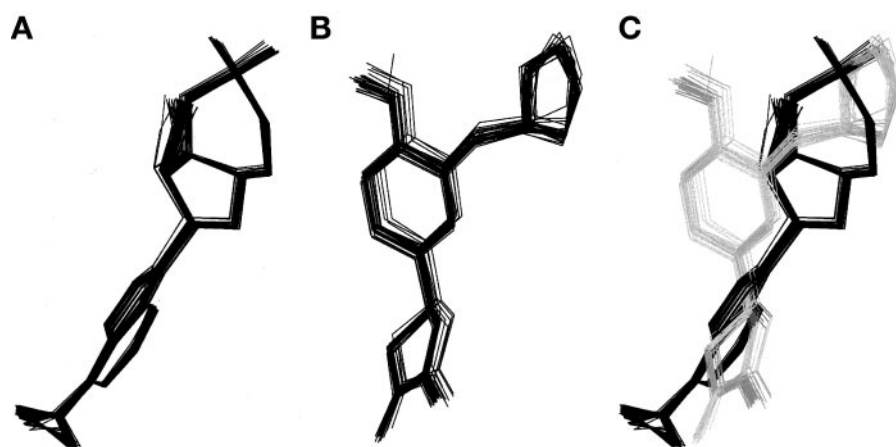
Fig. 1. Ensemble of cAMP and rolipram conformers docked in the binding pocket of PDE4, as obtained by the AutoDock program. A, cluster of 61 cAMP conformers with similar orientation. B, cluster of 32 rolipram conformers. C, superposition of cAMP cluster (61 conformers), shown in black, and rolipram cluster (32 conformers), shown in gray.

Asp392, and Met503, may play a role in rolipram binding based on predicted hydrogen bonds or van der Waals interactions (Fig. 2, A and B). Of these, Tyr233 has been identified as a critical residue in drug binding as a result of studies of the closely related PDE4A protein (Richter et al., 2001). The Y233F mutation reduced binding to rolipram by 140-fold. This mutation also has a profound effect on RP 73401 binding (reduced 1200-fold), which is consistent with our prediction that the tyrosine hydroxyl group participates in a hydrogen bond with the nitrogen atom of the drug. The fact that perturbations of these residues were not isolated in drug-resistance selections may reflect a less than exhaustive analysis or, in some cases, a low tolerance for substitutions at these sites when the detection of drug resistance requires that catalytic activity is intact.

It is noteworthy that all of the selected rolipram-resistance mutations are located within the region that is most highly conserved among PDE family members. Mutations giving rise to relatively minor reductions in rolipram sensitivity occurred at residues within helix $\alpha15a$ and are distal from the active site. The residues altered in the most drug-resistant mutants are located in helix $\alpha14$ and are part of subdomain 3. The exception to this clustering is Asp241, which, although nearby in three-dimensional space, is located in helix $\alpha6$ of subdomain one (Fig. 3). The $\alpha14$ residues involved in rolipram sensitivity form the lining of a tunnel located between helices $\alpha14$ and $\alpha6$ and lead to the deep active site pocket (arrow in Figs. 2A and 3). Moreover, their side chains are pointing toward the interior of the tunnel (Fig. 3). This configuration suggests that mutations in residues located within the tunnel may affect inhibitor entry and/or binding. This model is supported by the reduction in rolipram binding and sensitivity resulting from Asp241 mutants (D241A and D241N) (Pillai et al., 1993; Atienza et al., 1999). This residue is approximately 7 Å away from rolipram or cAMP (Table 1) and is therefore not expected to interact directly with them. Nevertheless, its side chain is pointing toward the tunnel; therefore, mutations of this residue might interfere with rolipram approaching the binding site.

It has been reported that PDE4 enzymes show an approximately 20-fold preference in binding to the R- versus the S-enantiomer of rolipram (Schneider et al., 1986; Underwood et al., 1993). Comparing hydrophobic and electrostatic interactions of the (R)- and (S)-rolipram conformations with the proposed binding site revealed a molecular basis for this observation. The two conformations (R and S) correspond to a rotation of the bond connecting C_5 and C_3. Manually flipping the pyrrolidinone moiety resulted in N_1's facing a different part of the protein (Fig. 2, B and C, respectively). Strikingly, this led to the prediction that for S-rolipram, a hydrophobic interaction with Trp406 and electrostatic contacts with Thr407 and Asn395 are lost, relative to the docked model of the R-enantiomer. Moreover, the positive charge on N_1 is not counter-balanced in the S-conformation, possibly resulting in destabilization.

In experimental systems, rolipram can display both high-affinity (nanomolar range) and low-affinity micromolar range) binding to PDE4 enzymes (Schneider et al., 1986; Torphy et al., 1992). The presence of a divalent cation (e.g., Mg^{2+}) in the active site seems to be involved in high-affinity drug binding as well as catalytic activity toward the substrate (Laliberte et al., 2000). The predicted site of cation binding places it ~2.6 Å from rolipram, which is within range to participate in direct interactions (with the pyrrolidinone ring) or water-mediated hydrogen bonding. Although no large conformational changes are believed to result from cation occupancy (Laliberte et al., 2000), it is possible that some localized perturbations could result in enhanced drug affinity.

We examined the configuration of two other established PDE inhibitors. RP 73401 (Ashton et al., 1994; Souness et al., 1995) is a highly potent PDE4-specific inhibitor. When docked into the PDE4 active site, 50 of the 100 conformers are situated too close to either Tyr233 or Cys499 residues. The remaining conformers are clustered into three general orientations, two of which are translated by ~2 Å with respect to each other (red and blue clusters in Fig. 5). In all three conformations, the cyclopentyloxy methoxyphenyl
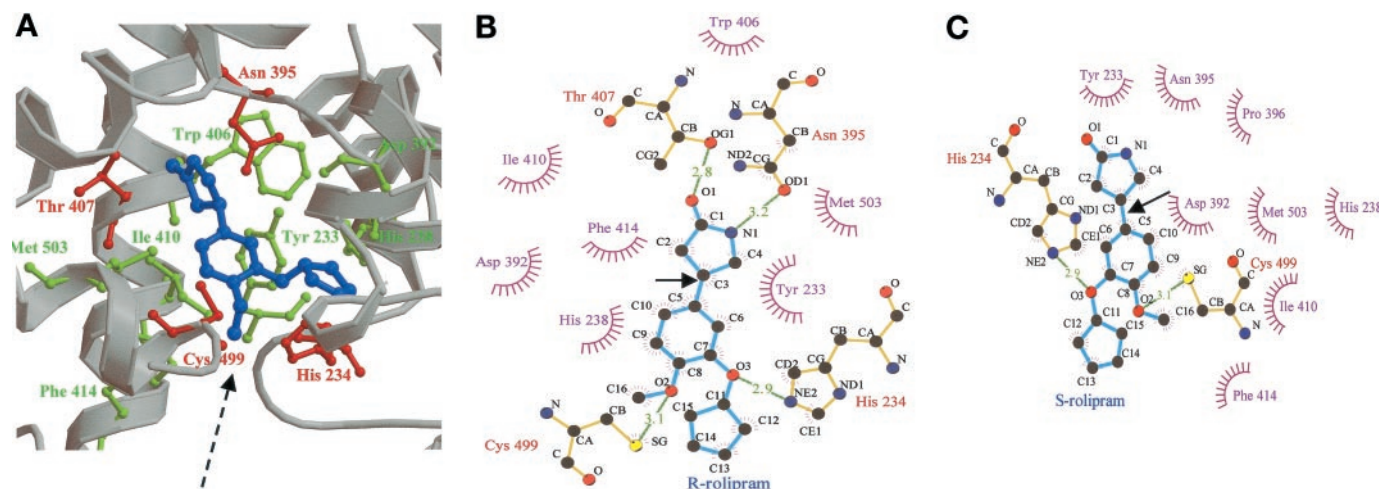
Fig. 2. Model of rolipram bound at the active site of PDE4. A, ball-and-stick representation of side chains predicted to interact through hydrogen bond (red) or hydrophobic contact (green) to rolipram (blue). A possible tunnel for substrate/inhibitor entry to the active site is shown as an arrow. B and C, schematic diagrams of PDE4 interactions with the docked (R)- and (S)-rolipram conformations, respectively, created using the program LigPlot (Wallace et al., 1995). The two conformations correspond to a rotation around the bond connecting C_5 and C_3 (arrow), flipping the pyrrolidinone moiety. Hydrogen bonds are presented as dashed lines, and the interatomic distances are shown in Ångstroms. The residues that form van der Waals contacts with docked rolipram are depicted as labeled arcs with radial spokes that point toward the ligand atoms with which they interact.

group of RP 73401 is adjacent to that of rolipram (when independently docked), suggesting that they share a similar orientation in the enzyme active site. Although the three RP 73401 conformers are not identical, they all display potential for multiple hydrogen bonds not found in rolipram. These additional interactions (with residues Asp275, Phe446, and Leu393) could form the basis for the increased potency of RP 73401. The existence of alternate, although closely related, binding configurations may also contribute to the observed high affinity and efficacy of this compound (a potentially useful conservation in drug design).

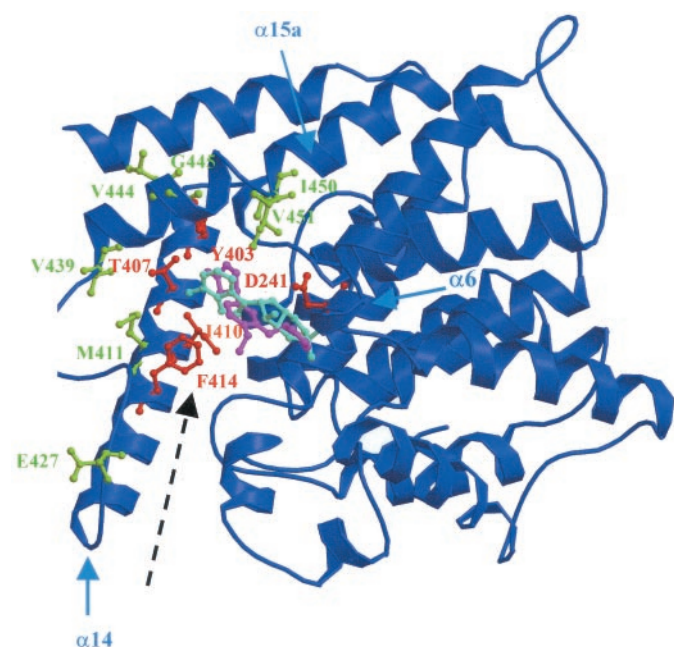3-Isobutyl-1-methylxanthine (IBMX) is a general competi-

Fig. 3. The active site pocket of PDE4B. Residues at which mutations can give rise to weak (green) or strong (red) resistance to rolipram are shown. The former are part of helix α15a and are distal from the active site. In contrast, the high drug resistance-conferring mutations are part of helices α6 and α14 and are in the vicinity of the substrate-binding pocket. The stick drawing of the consensus rolipram conformer (1 of 32) is depicted in magenta. The cAMP conformer (1 of 61) is in cyan. A possible tunnel for substrate/inhibitor entry to the active site is shown as an arrow.
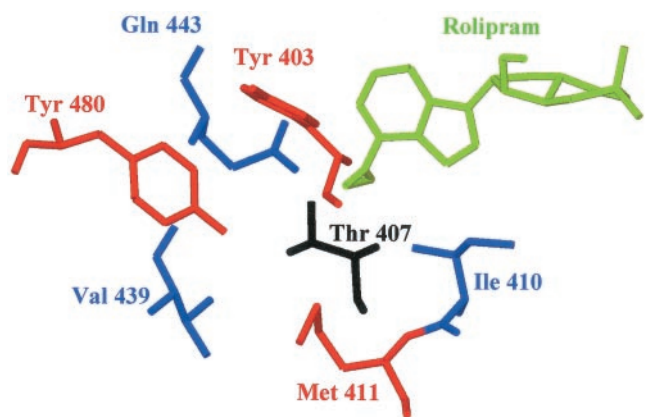

Fig. 4. Stick representation of the interactions between residue T407 and neighboring PDE4 residues and with the docked rolipram (green) consensus conformer. Residues that form hydrogen bonds to Thr407 (center) are depicted in red, and residues that form van der Waals contacts are depicted in blue.

tive inhibitor that works on most PDE isoforms but typically displays low affinity. For PDE4 enzymes, IBMX is a weak inhibitor, with IC_{50} values that are approximately 10-fold higher than the K_m value for substrate (Pillai et al., 1993; Atienza et al., 1999). This molecule is smaller than cAMP, rolipram, or RP 73401 and is too small to fill the available space in the active site. When docked into the active site, IBMX can adopt multiple conformations positioned in different places of the active site. Manual alignment of the common purine components of IBMX and cAMP, however, showed a loss of hydrogen bond interactions with both His238 and Asp392. These interactions involve the ribose phosphodiester moiety of cAMP for which there is no counterpart in IBMX. As a result, IBMX would be expected to show reduced binding affinity, in agreement with observation.

In conclusion, the cAMP and rolipram docked in the active site of PDE4 revealed that rolipram forms more van del Waals and electrostatic contacts with neighboring protein residues. This is in agreement with the observation that rolipram is found to be a PDE4-specific inhibitor that effectively competes with substrate. A correlation was observed between the net loss of electrostatic and van der Waals contacts of rolipram with protein residues and resistance to rolipram for the most affected mutants. The distribution of mutation sites suggests a possible molecular entry path for substrate and/or inhibitor to the active site. Furthermore, the PDE4 residues Tyr233, His234, Asp392, Ile410, and Cys499 are within hydrogen-bond distance or hydrophobic interactions with cAMP, rolipram, and RP 73401 atoms. These residues are located along the entry path to the active site (arrow in Fig. 2). On the other hand, Asn395 and Met503 are within hydrogen bond distance to rolipram and each of the three RP 73401 conformers but not to cAMP. Thus, it is reasonable to assume that the mutation of these residues could affect other PDE4 inhibitors. In addition, the increased sensitivity (lower IC_{50} value) for the R- versus S-conformation of rolipram can be explained, at least in part, by a

Fig. 5. Ensemble of the three RP 73401 conformer clusters docked in the PDE4 active site as obtained by using the AutoDock program. The three clusters contain 20, 19, and 12 conformers and are depicted in green, red, and blue, respectively.

diminished number of hydrophobic and hydrophilic contacts for the *S*-conformation. Finally, modeling of compounds with higher (RP 73401) or lower (IBMX) affinities for PDE4 has been used to provide insight into drug-enzyme interactions. These results, which represent the first working model for specific binding of phosphodiesterase inhibitors, should facilitate the further design and refinement of therapeutically useful compounds.

Acknowledgments

References

Ashton MJ, Cook DC, Fenton G, Karlsson JA, Palfreyman MN, Raeburn D, Ratcliffe AJ, Souness JE, Thurairatnam S, and Vicker N (1994) Selective type IV phosphodiesterase inhibitors as antiasthmatic agents. The syntheses and biological activities of 3-(cyclopentyloxy)-4-methoxybenzamides and analogues. *J Med Chem* **37:**1696–1703.

Atienza JM, Susanto D, Huang C, McCarty AS, and Colicelli J (1999) Identification of inhibitor specificity determinants in a mammalian phosphodiesterase. *J Biol Chem* **274:**4839–4847.

Barnette MS and Underwood DC (2000) New phosphodiesterase inhibitors as therapeutics for the treatment of chronic lung disease. *Curr Opin Pulm Med* **6:**164–169.

Cohan VL, Showell HJ, Fisher DA, Pazoles CJ, Watson JW, Turner CR, and Cheng JB (1996) In vitro pharmacology of the novel phosphodiesterase type 4 inhibitor, CP-80633. *J Pharmacol Exp Ther* **278:**1356–1361.

Conti M, Jin SL, Monaco L, Repaske DR, and Swinnen JV (1991) Hormonal regulation of cyclic nucleotide phosphodiesterases. *Endocr Rev* **12:**218–234.

Francis SH, Turko IV, and Corbin JD (2000) Cyclic nucleotide phosphodiesterases: relating structure and function. *Prog Nucleic Acid Res Mol Biol* **65:**1–52.

Goodford PJ (1985) A computational procedure for determining energetically favorable binding sites on biologically important macromolecules. *J Med Chem* **28:**849–857.

Goodsell DS, Morris GM, and Olson AJ (1996) Automated docking of flexible ligands: applications of AutoDock. *J Mol Recognit* **9:**1–5.

Holbrook M, Gozzard N, James T, Higgs G, and Hughes B (1996) Inhibition of bronchospasm and ozone-induced airway hyperresponsiveness in the guinea-pig by CDP840, a novel phosphodiesterase type 4 inhibitor. *Br J Pharmacol* **118:**1192–1200.

Houslay MD and Milligan G (1997) Tailoring cAMP-signalling responses through isoform multiplicity. *Trends Biochem Sci* **22:**217–224.

Jacobitz S, Ryan MD, McLaughlin MM, Livi GP, DeWolf WE, and Torphy TJ (1997) Role of conserved histidines in catalytic activity and inhibitor binding of human recombinant phosphodiesterase 4A. *Mol Pharmacol* **51:**999–1006.

Jin SL, Swinnen JV, and Conti M (1992) Characterization of the structure of a low Km, rolipram-sensitive cAMP phosphodiesterase. Mapping of the catalytic domain. *J Biol Chem* **267:**18929–18939.

Laliberte F, Han Y, Govindarajan A, Giroux A, Liu S, Bobechko B, Lario P, Bartlett

A, Gorseth E, Gresser M, et al. (2000) Conformational difference between PDE4 apoenzyme and holoenzyme. *Biochemistry* **39:**6449–6458.

Morris GM, Goodsell DS, Halliday RS, Huey R, Hart WE, Belew RK, and Olson AJ (1998) Automated docking using a Lamarckian genetic algorithm and an empirical binding free energy function. *J Comput Chem* **19:**1639–1662.

Owens RJ, Catterall C, Batty D, Jappy J, Russell A, Smith B, O'Connell J, and Perry MJ (1997) Human phosphodiesterase 4A: characterization of full-length and truncated enzymes expressed in COS cells. *Biochem J* **326:**53–60.

Pillai R, Kytle K, Reyes A, and Colicelli J (1993) Use of a yeast expression system for the isolation and analysis of drug-resistant mutants of a mammalian phosphodiesterase. *Proc Natl Acad Sci USA* **90:**11970–11974.

Raeburn D, Underwood SL, Lewis SA, Woodman VR, Battram CH, Tomkinson A, Sharma S, Jordan R, Souness JE, Webber SE, et al. (1994) Anti-inflammatory and bronchodilator properties of RP 73401, a novel and selective phosphodiesterase type IV inhibitor. *Br J Pharmacol* **113:**1423–1431.

Richter W, Unciuleac L, Hermsdorf T, Kronbach T, and Dettmer D (2001) Identification of inhibitor binding sites of the cAMP-specific phosphodiesterase 4. *Cell Signal* **4:**287–297.

Schneider HH, Schmiechen R, Brezinski M, and Seidler J (1986) Stereospecific binding of the antidepressant rolipram to brain protein structures. *Eur J Pharmacol* **127:**105–115.

Sippl W (2000) Receptor-based 3DQSAR analysis of estrogen receptor ligands—merging the accuracy of receptor-based alignments with the computational efficiency of ligand-based methods. *J Comput Aided Mol Des* **14:**559–572.

Soderling SH and Beavo JA (2000) Regulation of cAMP and cGMP signaling: new phosphodiesterases and new functions. *Curr Opin Cell Biol* **12:**174–179.

Souness JE, Maslen C, Webber S, Foster M, Raeburn D, Palfreyman MN, Ashton MJ, and Karlsson JA (1995) Suppression of eosinophil function by RP 73401, a potent and selective inhibitor of cyclic AMP-specific phosphodiesterase: comparison with rolipram. *Br J Pharmacol* **115:**39–46.

Spina D (2000) The potential of PDE4 inhibitors in asthma or COPD. *Curr Opin Invest Drugs* **1:**204–213.

Teixeira MM, Gristwood RW, Cooper N, and Hellewell PG (1997) Phosphodiesterase (PDE)4 inhibitors: anti-inflammatory drugs of the future? *Trends Pharmacol Sci* **18:**164–171.

Torphy TJ, Stadel JM, Burman M, Cieslinski LB, McLaughlin MM, White JR, and Livi GP (1992) Coexpression of human cAMP-specific phosphodiesterase activity and high affinity rolipram binding in yeast. *J Biol Chem* **267:**1798–1804.

Underwood DC, Osborn RR, Novak LB, Matthews JK, Newsholme SJ, Undem BJ, Hand JM, and Torphy TJ (1993) Inhibition of antigen-induced bronchoconstriction and eosinophil infiltration in the guinea pig by the cyclic AMP-specific phosphodiesterase inhibitor, rolipram. *J Pharmacol Exp Ther* **266:**306–313.

Wallace AC, Laskowski RA, and Thornton JM (1995) LIGPLOT: a program to generate schematic diagrams of protein-ligand interactions. *Protein Eng* **8:**127–134.

Xu RX, Hassell AM, Vanderwall D, Lambert MH, Holmes WD, Luther MA, Rocque WJ, Milburn MV, Zhao Y, Ke H, et al. (2000) Atomic structure of PDE4: insights into phosphodiesterase mechanism and specificity. *Science (Wash DC)* **288:**1822–1825.

Address correspondence to: John Colicelli, Department of Biological Chemistry, UCLA School of Medicine, 33–257 CHS, Los Angeles, CA 90095-1737. E-mail: colicelli@mednet.ucla.edu